International Forum on Aeroelasticity and Structural Dynamics
IFASD 2024
17-21 June 2024, The Hague, The Netherlands

# AEROELASTIC CHARACTERISTICS OF PLANE-SYMMETRY VEHICLE MAIN WING TRAILING EDGE RUDDER AT HIGH ANGLE OF ATTACK

**Li GUO[1], Yongde LI[1], Yingyu HOU[1], Junlin SHEN[1], Pu XING[1], Jue WANG[1],Chen JI[1,*]**

[1] Chinese Academy of Aerospace Aerodynamics, Beijing, 100074, China 1
[*]jichen167@hotmail.com

**Keywords:** plane-symmetry vehicle; aeroelasticity; stability of trailing edge rudder surface; large angle of attack

**Abstract:** The plane-symmetry shuttle vehicle experiences a long period of supersonic high angle of attack flight stage during its reentry. It is hard for the aerospace-vehicles structure to sustain long-time supersonic flight at high angle of attack. Therefore, the aeroelastic response characteristics of the trailing edge rudder surface of the typical plane-symmetric shuttle configuration require in-depth analysis. In this paper, the analysis and calculation of the trailing-edge rudder of at the high angle of attack is carried out in high speed. The numerical CFD/CSD coupling method is employed in the analysis. The calculation results show that the symmetrical and antisymmetric deflection modes of the trailing-edge rudder are unstable, and the aerodynamic damping identified by the ARMA method is less than 0, which indicates the aeroelastic instability. Therefore, the dynamic stability of the structure during the reentry period needs to be considered in the design of the plane-symmetric aircraft.

## 1 INTRODUCTION

Plane-symmetry reentry vehicles have the ability of two stage to orbit or even single state to orbit capabilities, which draws interests of aerospace applications. These kinds of Plane-symmetry reentry vehicles have the airplane-like abilities of flying in the atmosphere and space-ship-like abilities of reentry from outer space. And they have typical working condition differ from airplane, which include high flying speed and large angle of attack.

In large angle of attack condition, flow field and structures may have nonlinear effects, such as separation flows, boundary layer interacting with shock waves, and nonlinear aeroelastic interaction between flow field and structures. To account for the nonlinear effects, CFD method coupled with CSD is often used for aeroelastic simulations. McNamara et al. 1 use CFL3D program to predict the flutter boundaries of a control surface at Mach number 2.5~28 and compare the results with the prediction of piston theory. The differences between CFD/CSD prediction and piston theory is within 5% for the solely control surface cases. However, the differences amplify to 31% if influences of fuselage are taken into account. Aerodynamic heating would reduce the stiffness of structure material and introduce stress into the structure, which would reduce the flutter boundaries of hypersonic vehicles. Unevenly heating caused by large angle of attach would further reduce the flutter boundaries by 65%. Lamorte et al.2 simulate influences of real gas effects, turbulent model and transition position on flutter boundaries, and use a hypersonic vehicle control

surface as an example. The influence of real gas effect is less than 3% at 12km above the ground level and Mach number 13.7, which is negligible. Though flutter boundaries are insensitive to the changing of angle of attack at small angles, which has no obvious flow separation from the boundary layer, the flutter behavior at large angle of attack could be quite different. The detached flow from the wing surface could result in a significant change of fluid-structure interaction mode.

This work focused on the vehicles fluid-structure coupling behavior during large angle of attack, and using the numerical simulation method to find the stability characters.

## 2 BODY OF THE PAPER CHAPTERS

The analysis is about a in-house designed plane-symmetry reentry vehicle, with a body, 2 main delta-wings and tail rudders. A CFD-model coupling method is employed to simulate the fluid- structure coupling characters. Arbitrary Lagrangian-Eulerian equation (ALE) is used to describe the flow field on meshes moving with the deformation of the control surface. Mach number of the simulation is 5.0, and Reynolds number is $2.67\times10^7$. Angle of incoming flow is at 22°, and static pressure is 1617 Pa。 The flow field is approximately turbulence at this Reynolds number. Reynolds averaging Navier-Stokes (RANS) equation is employed to describe the averaged turbulence flow field. And Spalart-Allmaras (S-A) model3 is used to model the turbulence stress. In the simulation, density of the incoming flow is varying to exert different dynamic pressures on the structure. Speed of sound in the far-field and length of 1 meter are used to non-dimensionalize the equation. Roe scheme on cell centered unstructured meshes is used to discritize the space derivatives, and entropy correction is used to stabilize the calculation at hypersonic speed. In hypersonic flows, the time for flow passing the control surface is shorter than the structure vibration period. To increasing the time advancing stability when using large time step, dual-time stepping approach is used for time advancing. The mesh used in CFD simulation is shown in Fig. 1. Number of control volumes in the mesh is about $2.62\times10^7$, including $3.8\times10^5$ quadrilateral elements on the structure surface. Non-dimensional time step is $5.0\times10^{-3}$, which is 1/10 of the time span for fluids passing the control surface.

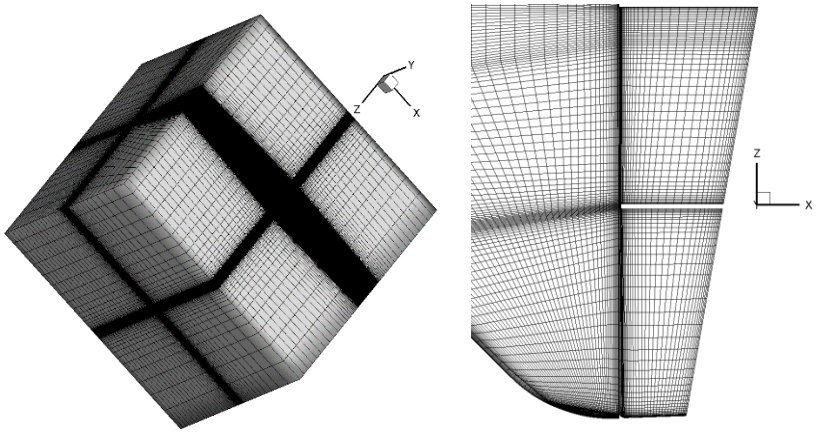


（a）far-field mesh　　b）mesh on the main wing surface

**Fig. 1. Computation domain and mesh distribution.**

Modes method is used to calculate the deformation of the structure. The *i*-th mode displacements $\boldsymbol{\psi}_i$ is normalized by its corresponding mode mass. Its frequency is $\omega_i$, and its mode coordinate is $z_i^{\psi}$. Structure displacement $\boldsymbol{z}$ in physical space is the summation of mode displacements timing their corresponding coordinate:

$$\boldsymbol{z} = \sum_i z_i^{\psi} \cdot \boldsymbol{\psi}_i .$$

Mode coordinates are obtained from the equation below:

$$\ddot{z}_i^{\psi} + \omega_i \cdot z_i^{\psi} = F_i .$$

where $F_i$ is the mode force, calculated by dot product of concentrated force on the structure nodes and corresponding mode displacement. Newmark method is used to advancing the equation of mode coordinates, and the time step is the same as the flow field calculation. Twenty modes are used in the simulation, including the main wing banding and flapping of the main delta-wing trailing edge rudder. Some mode shapes are show in Fig. 2. The frequency is non-dimensioned using income flow speed and character length.

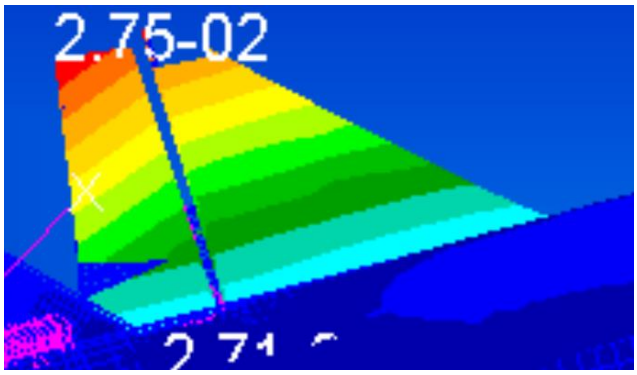


(a) bending mode of main wing ( ωb/v=7.01)

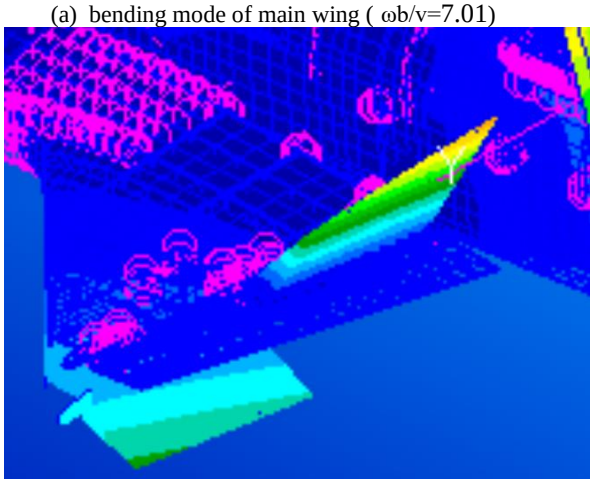

(b) flapping of main wing trailing edge rudder (ωb/v=8.99)

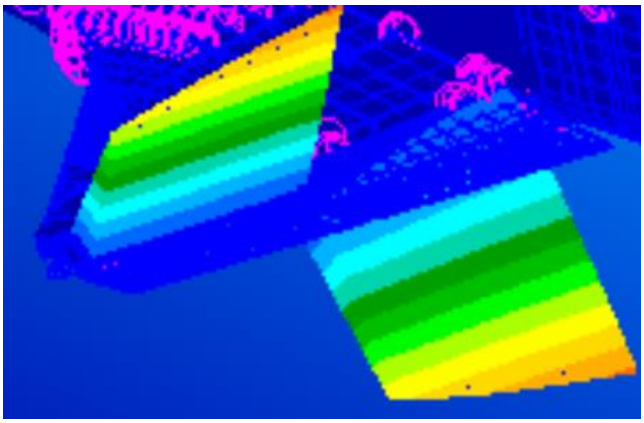

(c) flapping of main wing trailing edge rudder (ωb/v=21.76)

**Fig. 2. Mode displacements of the experiment model.**

Deformation of the control surface structure needs to be interpolated into the fluid mesh, and radial bases function (RBF) is used to do the interpolation. The value of RBF is only determined by the distance from the point to a reference point, and its values are no less than zero. If reference point on structure mesh is $\boldsymbol{X}_j$, the value of RBF $\eta$ on fluid mesh point $\boldsymbol{x}_i$ could be expressed as:

$$\eta = \eta\left(\left\|\boldsymbol{x}_i - \boldsymbol{X}_j\right\|\right)$$

Wendland C2 function is used as RBF function to interpolate the mesh deformation. In the function expression, reference length $\zeta_\phi$ is used to non-dimensionalize the distance variable $\zeta = \left\|\boldsymbol{x}_i - \boldsymbol{X}_j\right\| / \zeta_\phi$. Displacement $\Delta\boldsymbol{D}$ on fluid mesh point could be expressed as the summation of RBF and its corresponding weight $\boldsymbol{\alpha}_j$.

$$\Delta\boldsymbol{D}\left(\boldsymbol{x}_i\right) = \sum_j \boldsymbol{\alpha}_j \eta\left(\left\|\boldsymbol{x}_i - \boldsymbol{X}_j\right\| / \zeta_\phi\right).$$

The weight coefficient $\boldsymbol{\alpha}_j$ is determined by the displacement of the structure mesh, which has known from the structure deformation calculation. The amount of calculation needed to determine the interpolation coefficient $\boldsymbol{\alpha}_j$ is large, due to the ill conditioned matrix formed from the structure displacement. And a greedy method4 improved by Wang et al.4 is employed to alleviate the calculation burden.

In the calculation process, shape of boundary structure determines aerodynamic force distribution, and the aerodynamic forces influences the movement of the structure. The simulation is based on HUN3D **Error! Reference source not found.** CFD program, and structure dynamic simulation is added into the program as a module. The simulation of flow and structure vibration is carried out separately, and no uniform matrix is formed. Coupling of fluid and structures is implemented via data exchange during calculation. One way coupling of fluid and structures would incur instability and underestimate the fluttering boundaries. Predict-correct method has higher order of accuracy in time direction, and the resulted fluttering boundaries are more reliable. More intermediate steps could be added to predict-correct frame work to further increase the accuracy as shown in Fig. 3

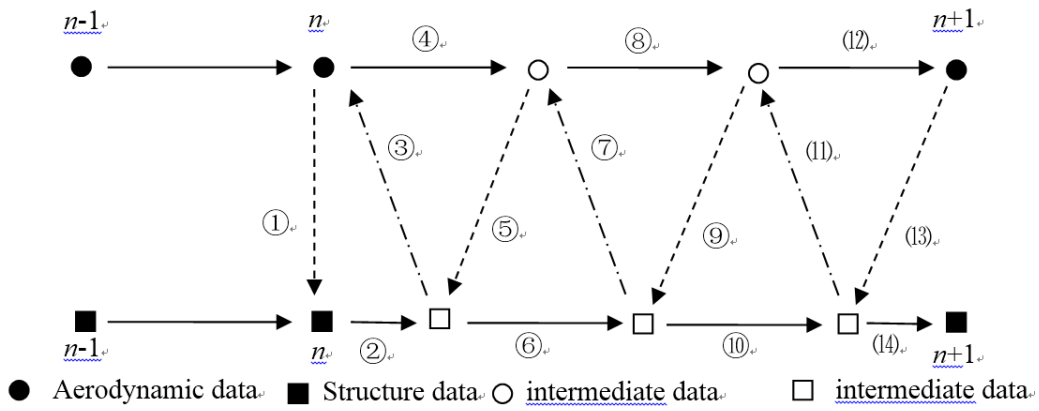


**Fig. 3. Predict-correct method with intermediate iterations**

Increasing the intermediate steps in coupling would need more mesh deformation interpolation, which is calculation dense. Though greedy method could increase the interpolation converging speed, the computation steal increases obviously. The main time consumption of interpolation is mainly from the determination of RBF coefficient. The displacements of the structure are varying from time to time, but the modes composing the displacement are the same. If the RBF coefficients for all modes displacement could be determined before the time advancing started in the initializing process and saved, the mesh deformation in every intermediate iteration would only involve dot production of mode coordinates and mode RBF coefficient, which is much more quick than calculating the coefficient directly from the structure displacement. The process is shown in Fig. 4.

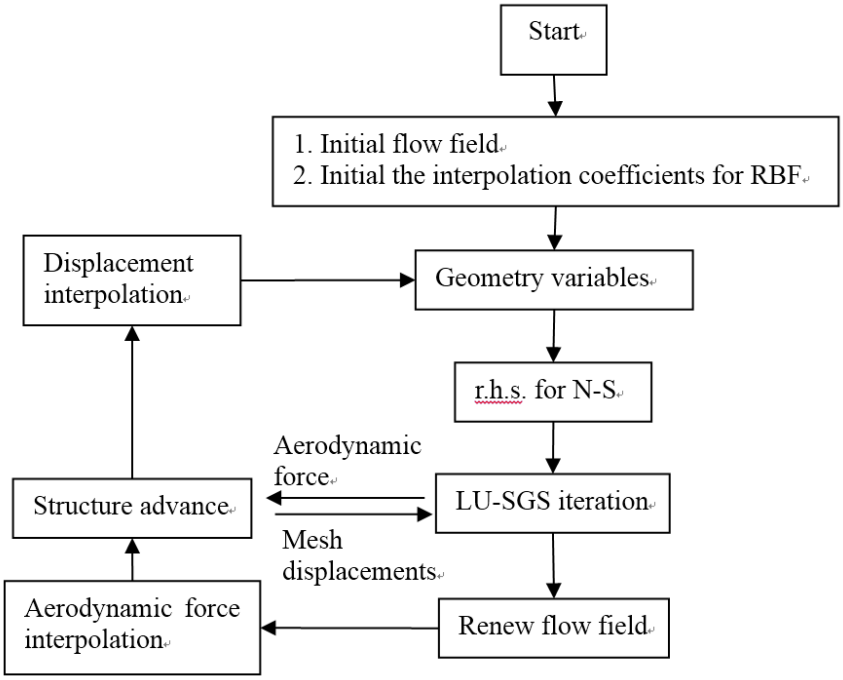


Fig. 4. Calculation procedure

## 3 RESULTS AND DISCUSSIONS

The flow vortex structure is shown in Fig. 5. The structure is dyed by the Mach number distribution. Strong streamwise vortex structures shedding from the main wing tips and trailing

edges of v-tails could be seen in Fig. 5. And local spanwise vortex structures is near the main wing elevator and front edge of the main wings. Complex vortex structures are at the back of the main body, which is formed by the abrupt ending of the main body.

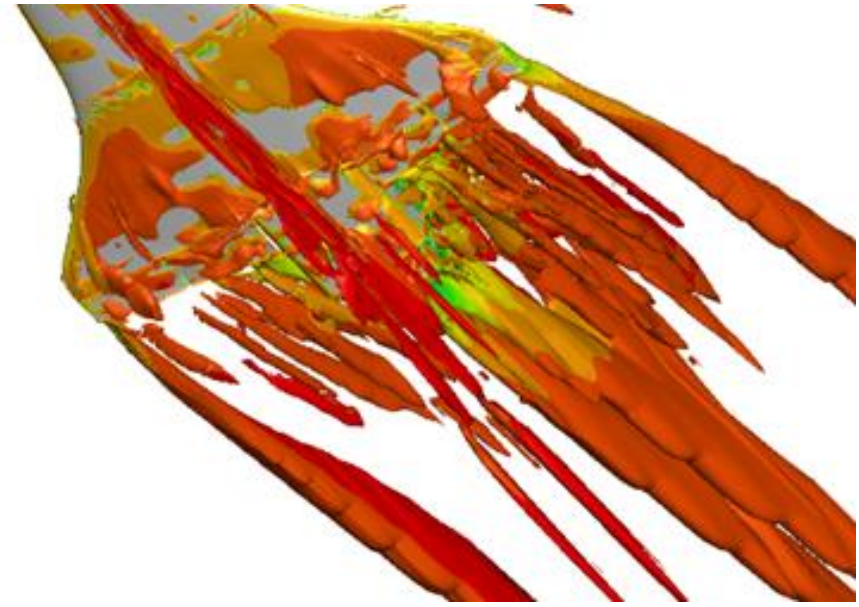

**Fig. 5 Vortex structure around the vehicle**

Generalized displacements of all the modes considered are checked for their stability. The only diverging mode is the ωb/v=22.76 last main wing trailing edge rudder flapping mode, with the shape shown in Fig. 2 (c). And other mods are converging. The time evolving history of the generalized displacement is shown in Fig. 6.

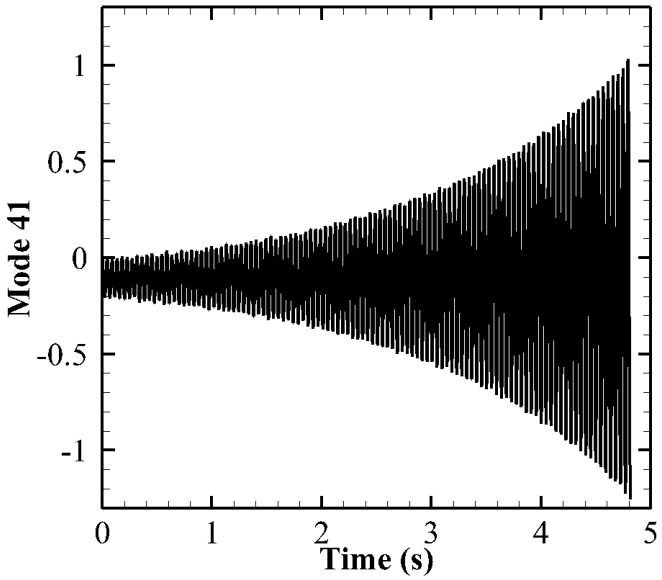


**Fig. 6 Generalized displacements of ωb/v= 22.76 last main wing elevator flapping mode**

ARMA (Auto-regressive Moving Average ) method is used to extract the vibration frequency and damping ration from the Generalized displacements of ωb/v=22.76 last main wing elevator flapping mode shown in Fig. 6. The damping ration is -0.46% and the frequency is ωb/v=22.09, which is only 2.9% different from the mode frequency ωb/v=22.76. As the changes of the diverging mode frequency from original frequency is small, the added aerodynamic mass and stiffness effect is not dominant. And the main reason of the divergence is the negative aerodynamic damping ratio, which is induced by the flow structures.

Fourier analysis of unsteady forces coefficients are carried out to find the character frequencies of the flow filed, which is shown in Fig. 7 and Table 1. Dragging coefficient has a character frequency of ωb/v=22.85. Lifting coefficient Cpy has both character frequency of ωb/v=22.85 and ωb/v=46.96. The main frequency of z-direction force coefficient is ωb/v=46.96. The divergence of the ωb/v=22.76 mode could be induced by the flow structures at the ωb/v=22.85 and ωb/v=46.96.

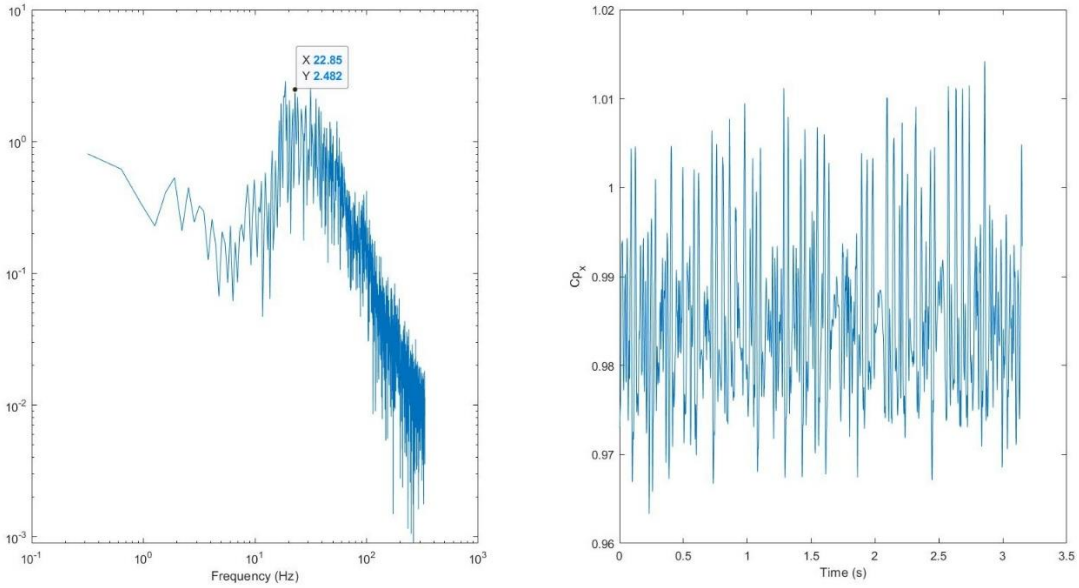


(a) Frequency domain and time domain dragging coefficient

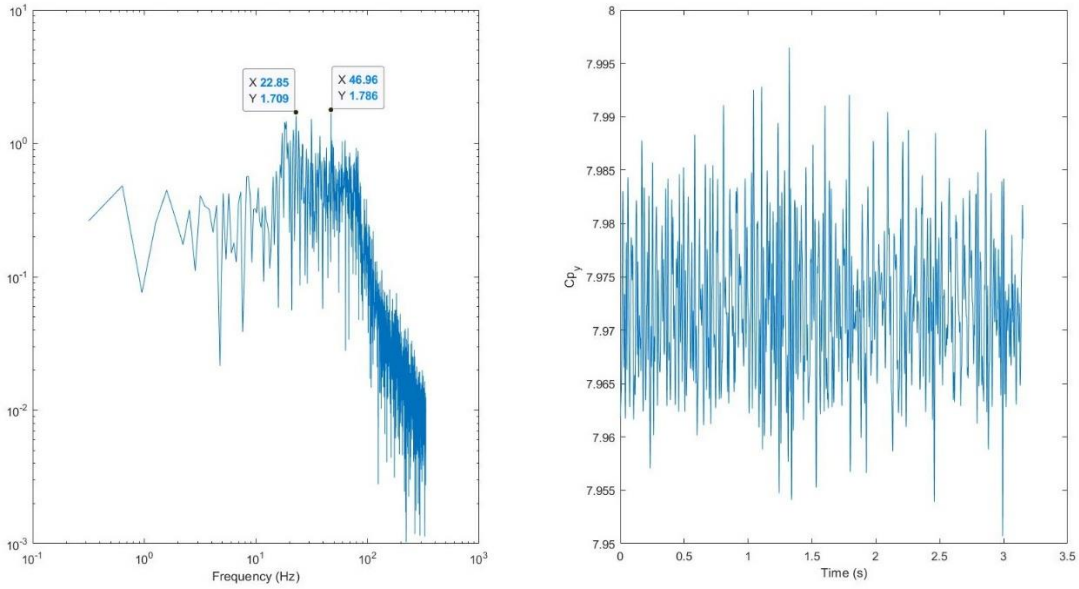


(b) Frequency domain and time domain lifting coefficient

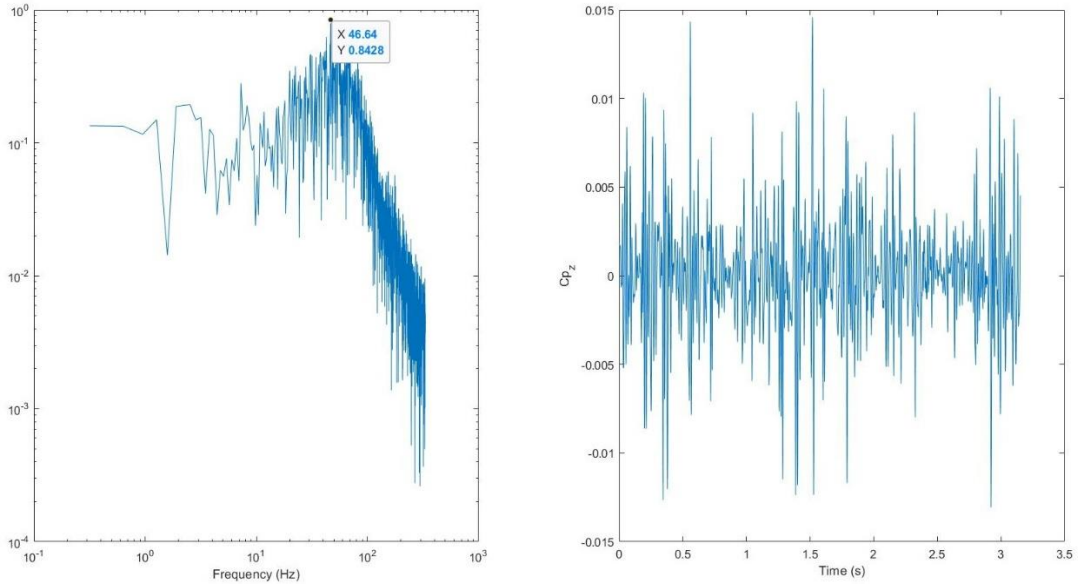


(c) Frequency domain and time domain z-direction force coefficient

**Fig. 7 Fourier analysis of force coefficients**

**Table 1 Frequencies of force coefficients**

| | 1st frequency（ωb/v） | 2nd frequency（ωb/v） |
|---|---|---|
| Dragging coefficient Cpx | 22.85 | -- |
| Lifting coefficient Cpy | 22.85 | 46.96 |
| z-direction force coefficient Cpz | -- | 46.64 |

Dynamic mode decomposition of the pressure on the vehicle surface is carried out to find the source of the frequencies from Fourier analysis. The DMD modes near the Fourier analysis frequencies are shown in Fig. 8. A flow structure mode of ωb/v=22.0 and ωb/v=45.0 could be extracted using the DMD analysis method. The mode of ωb/v=22.0 is mainly distributed spanwise and the mode of ωb/v=45.0 is mainly distributed streamwise.

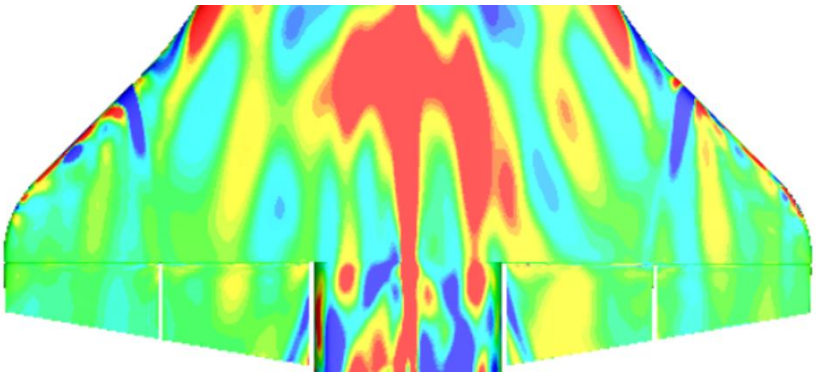

**（a） ωb/v=22.0 spanwise mode**

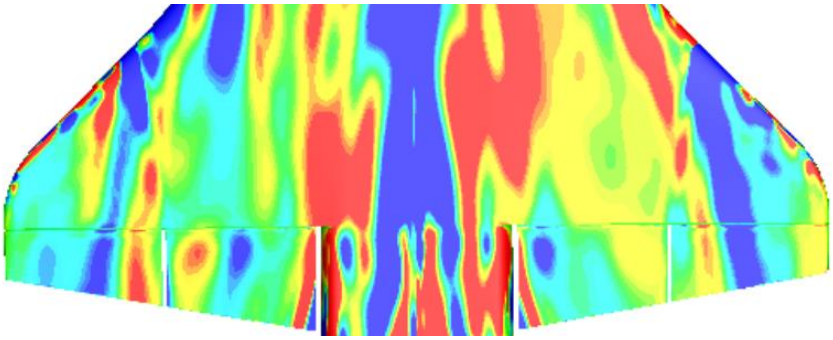

**（b） ωb/v=45.0 streamwise mode**

Fig. 8 DMD analysis of surface pressure distribution

## 4 CONCLUSION

An unstable flapping phenomenon is observed of an in-house plane-symmetry vehicle main wing trailing edge rudder at 22°angle of attack. It is analyzed in frequency domain and using DMD method to find that the unstable flapping mode is caused by the same frequency flow field DMD mode. The mode could induce -0.46% negative aerodynamic damping ratio into the fluid-structure coupling system, which cause the unstable divergence of the main wing trailing edge rudder flapping mode. And a structure damping ratio more than 0.46% could be used to suppress the divergence if needed.

## REFERENCES

1. [1] Jack J. McNamara, Peretz P. Friedmann, Kenneth G. Powell, Biju J. Thuruthimattam, Aeroelastic and Aerothermoelastic Vehicle Behavior in Hypersonic Flow, AIAA 2005-3305.
2. Nicolas Lamorte and Peretz P. Friedmann, Aerothermoelastic and Aeroelastic Studies of Hypersonic Vehicles using CFD, AIAA 2013-1591.
3. Spalart P R, Allmaras S R. A one-equation turbu-lence model for Aerodynamic flows, Le Recherche Aerospatiale, 1994, 1, 5-21.
4. Rendall T C S, Allen C B, Efficient mesh motion using radial basis functions with data reduction algorithms. Journal of Computational Physics. 2009(228), 6231–6249.
5. Wang G., Lei B., Ye Z., An Efficient Deformation Technique for Hybrid Unstructured Grid Using Radial Basis Functions, Journal of Northwestern Polytechnical University. 2011, 29(5). (in Chinese)

## COPYRIGHT STATEMENT